Thyroid

DOI: 10.1089/thy.2019.0196

Glis3 as a critical regulator of thyroid primordium specification

Giuditta Rurale[1,2], PhD, Federica Marelli[2], , PhD, Paolo Duminuco[1], BSc, Luca Persani[1,2], MD PhD

[1]*Department of Endocrine and Metabolic Diseases and Lab of Endocrine and Metabolic Research, Istituto Auxologico Italiano IRCCS, Milan 20149, Italy;* [2]*Department of Clinical Sciences and Community Health, University of Milan, Milan 20122, Italy*

Key words: Congenital Hypothyroidism; Thyroid Dysgenesis; Endoderm; Sonic Hedgehog; Thyroid Development; Zebrafish

Dr. Giuditta Rurale, PhD: giudi.rurale@gmail.com

Dr. Federica Marelli, PhD: federica.marelli@unimi.it

Dr. Paolo Duminuco, BSc: p.duminuco@auxologico.it

Prof. Luca Persani, MD PhD: luca.persani@unimi.it

Thyroid
Glis3 as a critical regulator of thyroid primordium specification (DOI: 10.1089/thy.2019.0196)

Abstract

Background: GLIS3 (GLI-Similar protein 3) is a transcription factor involved in several cellular processes. Homozygous mutations in the *GLIS3* gene have been typically associated with Neonatal Diabetes and Congenital Hypothyroidism (CH) in a syndrome called NDH. NDH patients present developmental abnormalities including endocrine pancreas defects and a spectrum of thyroid abnormalities, mainly including thyroid dysgenesis (TD). The mouse models revealed a key role of *Glis3* in pancreatic islets but not in early thyroid development, as *Glis3* was described to retain a role in regulating thyroid hormone synthesis downstream the TSH/TSHR signaling pathway and in postnatal follicle proliferation. Hence, in this study we have been taking advantage of the zebrafish model to gain insights on the Glis3 activity during thyroid organogenesis.

Methods: Transient *glis3*-knockdown zebrafish embryos (called *glis3* morphants) were generated by the microinjection of specific *glis3* morpholinos at 1-2 cells stage to analyze the thyroid phenotype *in vivo*. Several additional analyses (*in situ* hybridization, immunohistochemistry, pharmacological treatments) were performed for further molecular characterization.

Results: The analysis of thyroid embryonic development revealed that Glis3 is involved in early steps of thyroid specification. *glis3* morphants exhibited a reduced expression of the early transcription factors *nkx2.4* and *pax2a* at the thyroid primordium level, that is not caused by changes in proliferation or apoptosis of the pharyngeal endoderm. As a result, the differentiated thyroid tissue in morphants appeared reduced in size with decreased expression of *tg* and *slc5a5,* a low number of T4-producting follicles, associated with an elevation of *tshba* (homologous of the human TSHβ), thus resembling the clinical and biochemical manifestations of patients with TD. Interestingly, *glis3* morphants have pancreatic β–cell defects, but not liver defects. *In vitro* and *in vivo* data also demonstrated that Glis3 is an effector of the Sonic Hedgehog (SHH) pathway. Molecular and pharmacological inhibition of SHH reproduced the thyroid defects observed in *glis3* morphant.

Conclusions: Our results demonstrate that *glis3,* within the SHH pathway, appears to determine the number of endodermal cells committed to a thyroid fate. This is the first evidence of the involvement of Glis3 in TD, thereby expanding the understanding of the genetic basis of thyroid development and CH.

Thyroid
Glis3 as a critical regulator of thyroid primordium specification (DOI: 10.1089/thy.2019.0196)
This paper has been peer-reviewed and accepted for publication, but has yet to undergo copyediting and proof correction. The final published version may differ from this proof.

Introduction

Several key steps of thyroid development have been understood owing to the seminal work of several groups that identified the set of thyroid transcription factors that define the thyroid precursor cells as well as differentiated thyrocytes, but the mechanism underlying the specification of the thyroid *anlage* from the foregut endoderm are currently unknown (1-3).

The expression of *NKX2-1, PAX8, FOXE1* and *HHEX* is known to be required for adequate thyroid development and function in several models, including mice and zebrafish, and mutations affecting these genes have been associated with congenital hypothyroidism (CH), one of the most common congenital endocrine diseases and the most prevalent preventable form of mental retardation (1-6).

Recent findings indicate that the transcription factor GLI-Similar protein 3 (*GLIS3*) is a candidate gene for CH, although its role in thyroid pathophysiology remains largely unexplored. Homozygous and compound heterozygous mutations in *GLIS3* have been associated with a rare syndrome, referred to as NDH, characterized by neonatal diabetes (ND) and CH, and several additional features, including renal, hepatic and skeletal abnormalities (6-8). All NDH cases have low T4 and high TSH levels; at the level of the thyroid, they are associated with a broad spectrum of clinical manifestations ranging from dysgenetic defects (from athyreosis to hypoplasia) to functional defects with an *in situ* thyroid gland. Moreover, we identified a number of heterozygous *GLIS3* missense substitutions in a large cohort of patients with variable forms of CH (9). Interestingly, all of the *GLIS3* variants are associated with other rare mutations in genes involved in CH pathology, thus supporting the concept of a frequent oligogenic origin of CH (5, 6, 9).

GLIS3 is a component of Krüppel-like zinc finger nuclear transcriptional regulators, which share a highly conservation of five C_2-H_2-type zinc finger motifs (10). GLIS3 plays critical roles in development and function of several organs, controlling gene transcription through the binding with GLIS3-binding sites (G3BS) present in the regulatory regions of target genes. In humans, *GLIS3* is expressed in a tissue-specific manner, with abundant

expression in thyroid, pancreas, and kidney. The *GLIS3* gene generates several transcripts, some of which might have variable functional activities (10-12).

Up to now, the functional role of Glis3 has been extensively studied in mice. These monogenic diabetes models revealed that Glis3 is a fundamental player for endocrine pancreas differentiation from the endoderm, the definition of the β-cell mass, and that sustained postnatal expression is required for adequate insulin secretion and glucose metabolism (10, 13-16). In this context, several findings support the concept that Glis3 is one of the transcription factors belonging to the Sonic-Hedgehog (SHH) signaling pathway. In particular, the binding with the Suppressor of Fused (SUFU), a negative regulator of SHH, accounts for the stability and transactivation activities of GLIS3 (13-20).

As far as the thyroid gland is concerned, evidence from Glis3 knockout (KO) mice indicated that Glis3 is essential for TH biosynthesis and postnatal thyroid gland proliferation, acting down-stream of the TSH/TSHR system (10, 21). Although the size of the thyroid follicles is smaller in Glis3-KO pups in the first week after birth, the thyroid morphology and serum TH levels are similar compared to wild-type mice, suggesting that the development of CH in this particular Glis3-KO mouse is related to functional rather than developmental defects. These findings are in contrast to those observed in the NDH patients, in which thyroid dysgenesis is a common feature (7-9, 22).

In this study, we took advantage of the zebrafish model to characterize the role of Glis3 during early thyroid development. Zebrafish has emerged as a suitable model system in thyroid research, thanks to the high conservation of the molecular mechanisms involved in thyroid organogenesis, TH transport and metabolism, as well as TH action in target tissues (23-27). We previously described that the *glis3* transcript is detectable early during zebrafish embryonic development, and its signal depicts the foregut endoderm pouches, the tissue that will give rise to endocrine organs (e.g. thyroid and pancreas) (28). In the present work, we describe the effects of *glis3* knock-down (KD) in zebrafish. The multiple genetic and pharmacological manipulations demonstrate that *glis3,* within the sonic-hedgehog pathway, is a critical factor for the correct specification of thyroid primordium, likely regulating the number of endodermal cells committed to thyroid fate.

Thyroid
Glis3 as a critical regulator of thyroid primordium specification (DOI: 10.1089/thy.2019.0196)
This paper has been peer-reviewed and accepted for publication, but has yet to undergo copyediting and proof correction. The final published version may differ from this proof.

Thyroid
Glis3 as a critical regulator of thyroid primordium specification (DOI: 10.1089/thy.2019.0196)

Materials and Methods

Ethical statement

Current Italian national rules: no approval needs to be given for research on zebrafish embryos. Fish were maintained and raised according to EU regulations on laboratory animals (Directive 2010/63/EU).

Zebrafish line and maintenance

Wild-type adults (AB strain) were obtained from the Wilson lab, University College of London, UK, and maintained in a flow-through system in charcoal-filtered tap water at a constant temperature (28±1°C), with a photoperiod of 14:10 (light:dark). Zebrafish embryos, obtained from natural spawning, were raised and maintained according to established techniques (29, 30), and staged according to morphological criteria (31). Beginning from 24 hours post fertilization (hpf), the embryos were cultured in fish water containing 0.002% of 1-phenyl-2-thiourea (PTU, SIGMA) to prevent pigmentation, and 0.01% methylene blue to prevent fungal growth. Such a low dose of PTU (0.002%) does not affect TH synthesis and the thyroxine concentrations are similar in treated and untreated fish (32). The Wild Type (WT) AB strain zebrafish line was used.

Probes preparation and whole mount in situ hybridization (WISH)

For *glis3* (ENSDART00000142833.2) antisense digoxigenin (DIG) probe synthesis, a 1024 bp template was generated by RT-PCR on total RNA extracted from pools of embryos at 26-48 hpf. The primers used for probe amplification are the following: FW: 5' TGGGAAAGGCTGTAACCTGA 3' and REV: 5' GGACACCTCAAACTGAAGCG 3' (28, 33). The PCR products were cloned into the pCRII-TOPO vector (Invitrogen, Carlsbad, CA) and the cDNA-containing plasmids were enzymatically linearized and *in vitro* transcribed to antisense digoxigenin (DIG) riboprobes using T7 or SP6 with RNA polymerase (Roche).

The riboprobes against *nkx2.4, pax2a*, *tg, slc5a5* (33), *tshba* (34), *shha (35)*, *foxa2* (36)*, isl1* (37)*, foxa3* (38)*, ptf1a* (39)*, ins2* (40) mRNAs were used to evaluate thyroid, endoderm, liver and pancreas development and function. WISH experiments were performed according to Thisse *et al*. (41). Depending on the experiment, the DIG-probes were

Thyroid
Glis3 as a critical regulator of thyroid primordium specification (DOI: 10.1089/thy.2019.0196)

detected using anti-DIG-alkaline phosphatase (AP) and NBT/BCIP or Fast Blue. For the analysis of thyroid volume quantification (NBT/BCIP), the embryos were flat mounted, and the number of positive cells was calculated by dividing the area of positive staining by the average area of a single cell using ImageJ software (http:// rsb.info.nih.gov/ij/). The double fluorescent WISH was performed as previously described (42). The DIG- and FLUO-labelled probes were either revealed by Fast Blue and Fluorescein using the Perkin Elmer TSA kit. The fluorescent signals were detected by confocal microscopy and the fixed embryos were embedded with 80% glycerol and mounted on glass slides. Stacks were recorded using a 20x objective plus 2x zoom (Nikon C2+ confocal system; Nikon) and the images were processed using Adobe Photoshop CS2.

Loss-of function analysis

The embryos were injected with a specific Morpholino (MO), a specific antisense oligonucleotide to transiently knock down the gene function.

The specific *glis3* morpholino (*GLIS3*MO_SPL: 5' TTCTTGTTTTTACCTTTCATACCGC 3') was designed by Gene Tools (LLC, Philomath, OR), in order to recognize the splice donor site of the exon 2-intron 2 boundary of the pre-mRNA. The negative controls were generated by the injection of standard control morpholino (std ctrl-MO: 5' CCTCTTACCTCAGTTACAATTTATA 3') that targets the human *β-globin* gene. Morpholinos were dissolved in Danieau's buffer (58 mM NaCl; 0.7 mM KCl; 0.4 mM $MgSO_4 \cdot H_2O$; 0,6 mM $Ca(NO_3)_2$; 5 mM Hepes pH 7.2). Embryos were microinjected at the 1–2 cells stage and Rodamine dextran (Molecular Probes) was usually co-injected as a tracer.

The *GLIS3*MO_SPL was validated by RT and qRT –PCR. Total RNA was extracted from injected and control embryos at 1 and 2 days post-fertilization (dpf) using TRIzol™ (Thermo Fisher Scientific). The reaction was carried out following the protocol of GoScript™ Reverse Transcription System (Promega). The cDNAs were then subjected to PCR amplification using GoTaq polymerase (Promega) following the manufacturer's instructions. Quantitative real-time PCR (qRT-PCR) was performed by ABI PRISMTM 7900HT Fast Real-Time PCR System using SYBRGreen MasterMix (Invitrogen). A second *glis3* splicing morpholino (43) (*GLIS3*_MO2: 5'ACCTGCTGCAAGAGATCAGTTAAAA 3') has

been used to confirm the results obtained with the *GLIS3*MO_SPL. The *shha*_MO (44) (5'CAGCACTCTCGTCAAAAGCCGCATT3') was used to investigate the relationship between glis3 and Shh.

Rescue experiments

Full-length zebrafish wild type *glis3* cDNA was cloned into the pcs2^{+} vector (Invitrogen), using the following primers: *glis3*CDS_FW: 5' ATGGACATGAATGGGAAAG 3' and *glis3*CDS_REV: 5' TCAGCCTTCAGTGAACACACA 3'.

The mutated form of *glis3* mRNA was generated introducing a point mutation GGA>TGA at position 1223 bp that causes the formation of a premature stop codon upstream of the zinc-finger functional domain. Both constructs (WT and MUT) were linearized and *in vitro* transcribed using the mMessage mMachine Sp6 kit (Thermo Fisher Scientific), following the manufacturer's instructions. The GFP mRNA was used as control for *glis3* mRNAs microinjection, which has no targets in zebrafish.

Immunofluorescence

The qualitative analysis of TH production was performed by immunofluorescence according to standard procedures using a rabbit anti-T4 BSA serum (1:1000; ICN Biochemicals) and the AlexaFluor 555 anti-rabbit IgG as secondary antibody (1:500, Life Technologies) (23, 36).

To test proliferation and apoptosis, after WISH with *nkx2.4*-DIG riboprobes and Fast Blue staining, embryos were stripped and rinsed in PBS. Anti-phospho-histone H3 (PH3) and antiactive caspase-3 (AC-3) antibodies (1:250; Cell Signaling) were used as primary antibodies, followed by incubation with an antirabbit IgG secondary antibody/AlexaFluor 488 (1:500; Life Technologies) (36).

Immunocytochemistry

The entire CDS of the zebrafish *sufu* and *glis3* were amplified and cloned into the pEGFP-C3 and pcDNA4-Myc/His, respectively. HeLa cells were transfected with 1 µg of pEGFP_sufu or pcDNA4-Myc/His-glis3 plasmids (0.5µg each in co-transfection assay). After

Thyroid
Glis3 as a critical regulator of thyroid primordium specification (DOI: 10.1089/thy.2019.0196)
This paper has been peer-reviewed and accepted for publication, but has yet to undergo copyediting and proof correction. The final published version may differ from this proof.

Thyroid
Glis3 as a critical regulator of thyroid primordium specification (DOI: 10.1089/thy.2019.0196)
This paper has been peer-reviewed and accepted for publication, but has yet to undergo copyediting and proof correction. The final published version may differ from this proof.

24 h, the transfected cells were fixed with 4% paraformaldehyde (Sigma-Aldrich), permeabilized with 0.1% Triton X-100 (Sigma-Aldrich). For the detection of the glis3 construct, the cells were incubated o.n. with α-c-Myc primary antibody (1:100; Life Technologies) and than detected with secondary antibody Alexa Fluor 555 goat anti-mouse IgG, (1:500 Life Technologies). The fixed cells were mounted with Slow-Fade Gold antifade reagent with DAPI (Life Technologies) and acquired using the Nikon Eclipse Ti confocal microscope equipped with a 60× oil immersion objective.

Co-immunoprecipitation

HeLa cells were transfected as previously described and after 24 h, the total protein content was extracted using Cell Lysis Buffer (20 mM Tris–HCl pH 7.5, 150 mM NaCl, 1 mM EDTA, 1 mM EGTA, 1% Triton X-100, protease inhibitor cocktail (Roche)), and sonication. Protein lysates were quantified by BCA protein assay (Thermo Fisher Scientific) and 300 µg of protein sample was incubated for 45 min RT with 450 µg of Dynabeads^{TM} Protein G (Invitrogen) conjugated to 1 µg of anti-c-Myc Monoclonal Antibody (Invitrogen) or 1 µg of normal mouse IgG (Santa Cruz Biotechnology). Magnetic beads were washed four times in PBS with 0.02% Tween-20, and resuspended in 20 µl 2x sample loading buffer (50 mM Tris-HCL pH 6.8, 2% SDS, 0.1 % bromophenol blue, 10% glycerol) and 200 mM DTT (Sigma-Aldrich). Immunocomplexes and input fractions were examined by Western blot using 4-12% NuPAGE Bis-Tris pre-cast polyacrylamide gels (Thermo Fisher Scientific). Immunoblots were performed with mouse c-Myc antibodies (1:500 Life Technologies) or mouse GFP antibody (1:1000, Origene) diluted in 5% milk in TBS with 0.1% Tween-20 (Sigma-Aldrich).

Cyclopamine treatment

For the inhibition of the Shh pathways, from 50% epiboly stage to 26 or 48 hpf, the embryos were treated with 10 µM Cyclopamine (Sigma-Aldrich) harvested in fish water (45, 46); 1%DMSO (dimethylsulfoxide) was used as a control vehicle.

Statistical analysis

All data are shown as means ± standard deviation (SD) or percentages. The *t*-student test was used for the analysis of differences between groups. The $p < 0.05$ was considered

statistically significant. All the analyses were conducted with the software package GraphPad Prism 4.0 (GraphPad, San Diego, CA).

Results

glis3 knockdown affects the specification of thyroid primordium

Knockdown experiments were performed by the microinjection of a specific *glis3* morpholino (*glis3*MO_SPL) into zebrafish embryos (called morphants). Following the set-up of *glis3* gene knockdown and embryonic phenotype analysis (see Supplementary, section 1), we performed whole mount *in situ* hybridization to test whether *glis3* plays a role in zebrafish thyroid organogenesis.

At 1 dpf, the thyroid primordium was defective with a marked reduction of *nkx2.4* and *pax2a* expression in the *glis3* morphants (Fig 1A-C' and E-G'). The *nkx2.4* was markedly reduced in the thyroid bud compared to controls in 65.6% of embryos injected with 0.3 pmol/e of *glis3*MO_SPL, and undetectable in almost all the embryos injected with 0.5 pmol/e of *glis3*MO_SPL (Fig 1D). Consistently, a reduced to absent *pax2a* expression was seen in 17.6% to 33.9%, respectively, of the embryos injected with 0.3 pmol/e MO, and the expression of *pax2a* was reduced to absent in the 31.2% and 68.8% of morphants injected with 0.5 pmol/e (Fig 1E-H). When compared with the size in control embryos, the volume of the thyroid primordium was reduced by 50-95% in morphants (Fig 1 Graphs D' and H').

The mechanisms underlying the altered thyroid phenotype in the *glis3*-knockdown embryos was investigated by activated caspase-3 (AC-3) or phospho-histone H3 (PH3) immune-staining as markers of apoptosis or proliferation, respectively (Fig 1I-L). At 1 dpf, no significant differences in AC-3 (Fig I-J) or PH3 (Fig 1K-L) staining were seen by confocal microscopy in the area of *nkx2.4* expression in all morphants. These findings indicate that the reduced expression of the early thyroid markers is not associated with a decreased proliferation nor an increased apoptosis of the endoderm precursors committed to thyroid fate. In aggregate, these findings point to the potential role of *glis3* in regulating the amount of endoderm cells that will be addressed to thyroid precursors.

Thyroid
Glis3 as a critical regulator of thyroid primordium specification (DOI: 10.1089/thy.2019.0196)
This paper has been peer-reviewed and accepted for publication, but has yet to undergo copyediting and proof correction. The final published version may differ from this proof.

glis3 morphants have thyroid dysgenesis and primary hypothyroidism

At 2 dpf, the precursors of thyroid primordium differentiate into thyroid follicles, expressing the functional markers *tg* and *slc5a5*, and proliferation along the ventral aorta by 3 dpf (26). In agreement with the findings reported above, the injection of 0.3 pmol/e or 0.5 pmol/e MO caused a marked and dose-dependent reduction of all the examined markers. The *tg* transcript was reduced in 51.7% and 74.4% of morphants, respectively (Fig 2A-C). Similarly, the *slc5a5* transcript was reduced, frequently below the limit of detection, in 74 or 88% of morphants (Fig 2D-G). At 3 dpf, the thyroid gland elongates along the midline forming the classical V-shape (Fig 2H): the staining of *tg* continued to be reduced in 32 or 50% of the morphants (Fig 2I and K). Interestingly, a significant portion of morphants exhibited a normal expression of *tg,* but their thyroid follicles were disorganized and ectopically displaced along the ventral aorta (Fig 2J and K).

The quantification of tg+ cell number confirmed the distribution of the thyroid phenotype of *glis3* morphants at 2 and 3 dpf (Fig 2L and M).

A double fluorescent WISH of early and late thyroid markers was also performed to understand the variable degree of impairment detected in the in *glis3* morphants up to 60 hpf (see Supplementary, section 2). Most of the embryos presented a significant reduction of both early transcripts (*nkx2.4* and *pax2a*), but *pax2a* was generally diminished to a larger extent. However, when the expression was completely absent, no thyroid bud was present and all markers were affected.

Immune-staining with an anti-T4 antibody was performed to assess the status of thyroid function at 5 dpf by comparing the control and morphants injected with 0.5 pmol/e. By counting individual T4-positive follicles, we observed that the *glis3* morphants exhibited a significantly (p<0.01) reduced number of follicles (n: 3±1 vs 5±1) (Fig 2N-P). Consistently, 85% of the *glis3* morphants presented a significant increase (p<0.001) in the number of the *tshba* (homologous of human *TSHβ*) positive pituitary cells at 5 dpf (n: 13±2 vs 4±1) (Fig 2Q-S).

The low T4 production and the high *tshba* expression observed in *glis3*-knockdown larvae well recapitulate the clinical findings described in patients with thyroid dysgenesis. The

thyroid phenotype in *glis3*-deficient embryos was faithfully confirmed by using a second *glis3* splicing morpholino that had been previously validated (43) (see Supplementary, section 3).

The glis3 gene dosage regulates the number of the differentiated thyroid follicles

To confirm the specific thyroid phenotype resulting from *glis3* morpholino activity, we performed mRNA rescue experiments co-injecting the *glis3*MO_SPL with the wild-type or mutated zebrafish *glis3* transcripts. The mutant *glis3* mRNA was generated introducing a point mutation GGA>TGA at position 1223, that causes the formation of a premature stop codon upstream of the ZF domain, mimicking natural human *GLIS3* mutations (7).

The co-injection with the *glis3*MO_SPL and the *glis3*_WT mRNA was able to rescue the loss of expression of *nkx2.4* and *tg* (Fig 3D and D') induced in the vast majority of the embryos injected with *glis3*MO_SPL alone (Fig 3C and C'). Interestingly, the co-injection of the *glis3*MO_SPL and the *glis3*_MUT mRNA (Fig 3E and E') failed to rescue the thyroid defects of *glis3* morphants and even worsened the phenotype. The thyroid was not affected after the injection of the same doses (100 pg/e) of WT or MUT *glis3* mRNAs (Fig 3B and B').

To further define whether *glis3* gene dosage contributes to the onset of thyroid defects, we performed over-expression experiments microinjecting growing doses of *glis3*_WT mRNA. When compared with controls at 2 dpf (Fig 3F), the injection of 250 pg/e of the *glis3*_WT mRNA was associated with an upregulation of *tg* expression in 75% of embryos, and an enlargement of the thyroid *anlage* (+130% than controls) (Fig 3H and I). Confirming the previous results, the thyroid was smaller in 87% of *glis3* morphants compared to controls (Fig 3G and I), and the number of T4-producing follicles was reduced by 50% (Fig 3F' and G'). In contrast, the overexpression of *glis3* led to a significant increase of the T4 production (Fig 3H' and I').

To test whether the increased size of the thyroid gland in the *glis3*-overexpressing embryos was caused by an increased proliferation in the foregut endoderm or an enlarged number of endodermal cells committed to the thyroid fate, we performed proliferation assays at different time points. Since no differences in phospho-histone H3 levels were detected in the pharyngeal floor in early and late developmental stages after the injection

Thyroid
Glis3 as a critical regulator of thyroid primordium specification (DOI: 10.1089/thy.2019.0196)
This paper has been peer-reviewed and accepted for publication, but has yet to undergo copyediting and proof correction. The final published version may differ from this proof.

of 250 pg/e *glis3*_WT mRNA (Fig 3J-O), these data also support the concept that the amount of *glis3* activity is critical for the determination of thyroid primordium size.

glis3 regulates the development of the endoderm-derived endocrine organs

In order to exclude a global impairment of the pharyngeal endoderm in the *glis3* morphants, we analyzed the expression of *foxa2*, an early endoderm-specific transcription factor. When thyroid bud becomes evident (22hpf), the endoderm pouches appeared unaffected in *glis3* morphants (Fig 4A and B).

Furthermore, we investigated whether other endoderm-derived organs, such as liver and pancreas, show developmental defects in *glis3* morphants. Liver development was unaltered in 100% of the *glis3* morphants, as shown in the WISH analysis of the expression of the liver-specific genes *isl1* and *foxa3* (Fig 4C-F). In contrast, the *glis3* morphants showed endocrine pancreas defects (Fig 4G-I). In 52% of morphants we observed an impaired *ins2* expression at 2 dpf (Fig 4H), and in the remaining 48% the *ins2* expression was disorganized, i.e. the insulin2-positive cells failed to converge on the midline to form a single islet (Fig 4I). The WISH of the acinal specific marker *ptf1a* also confirmed that the pancreatic defects of morphants were restricted to the endocrine compartment (see Supplementary, section 4).

These results suggest that *glis3* action is required for the correct development of the thyroid and the endocrine pancreas, but its down-regulation does affect the formation of pharyngeal endoderm pouches and liver development.

glis3 acts as an effector of the sonic-hedgehog pathway

Preliminary *in vitro* assays confirmed that sufu and glis3 interact even in zebrafish, since they co-localized and co-immunoprecipitated in a protein complex (see Supplementary, section 5).

To study the relationship between *glis3* and Shh, the expression of *shha* was analyzed in *glis3* morphants by WISH. When compared with controls at 2 dpf (Fig 5A and B), the 100% of *glis3* morphants injected with 0.5 pmol/e, presented a significant reduction of *shha* expression in the pharyngeal endoderm (Fig 5C and D).

Thyroid
Glis3 as a critical regulator of thyroid primordium specification (DOI: 10.1089/thy.2019.0196)
This paper has been peer-reviewed and accepted for publication, but has yet to undergo copyediting and proof correction. The final published version may differ from this proof.

Thyroid
Glis3 as a critical regulator of thyroid primordium specification (DOI: 10.1089/thy.2019.0196)
This paper has been peer-reviewed and accepted for publication, but has yet to undergo copyediting and proof correction. The final published version may differ from this proof.

The expression of *glis3* was previously shown to be expressed early in the pharyngeal endoderm and absent in the differentiated thyroid (28). Here, we show that the downregulation of the shh pathway by injection of *shha*_MO (1.25 pmol/e) (44) or treatment with cyclopamine (10 µM) (45, 46) is associated with the lack of *glis3* expression in both brain and pharyngeal endoderm (Fig 5E-L).

To test whether Shh signalling plays a role in thyroid development, the expression of endodermal and thyroid markers was analyzed by WISH in the cyclopamine treated embryos. In agreement with the key role of the shh pathway during endoderm formation and development, *foxa2* was compromised in the cyclopamine-treated embryos (Fig 6A and B). As a consequence of the pharmacological inhibition of the shh pathway, thyroid development was severely compromised. In fact, at 1 dpf, *nkx2.4* and *pax2a* signals were reduced/absent at the level of thyroid primordium in the 100% of the cyclopamine-treated embryos (Fig 6C-F), and at 2 and 3 dpf, *tg* expression was reduced in 68% or absent in 32% of treated-embryos (Fig 6G-L).

The overexpression of *glis3* after the injection of WT *glis3* mRNA (250 pg/e) did not alter *shha* transcript levels at 2 dpf (Fig. 6M and N), but enhanced the number of endodermal precursor cells toward the thyroid fate, thus resulting in an excess of *tg*-expressing cells (Fig 3). Surprisingly, cyclopamine treatment is able to completely counteract the effects of *glis3*-overexpression, and thus negatively affects thyroid development (Fig 6O-Q). Accordingly, *glis3* requires shh signaling for its activity and is likely to be a main downstream effector of this pathway in thyroid specification.

Discussion

Here, we demonstrate that the down-regulation of *glis3* in zebrafish embryos leads to developmental defects in the thyroid, replicating the thyroid dysgenesis reported in several patients with *GLIS3* mutations. The step-by-step analysis of thyroid organogenesis reveals that *glis3* knockdown interferes with the specification of thyroid precursors from the pharyngeal endoderm, as shown by the absent or reduced expression of the early transcription factors *nkx2.4* and *pax2a* at 1 dpf. Interestingly, at early stages of development the *glis3* knockdown appears to affect *pax2a* to an extent larger than *nkx2.4.*

Thyroid
Glis3 as a critical regulator of thyroid primordium specification (DOI: 10.1089/thy.2019.0196)
This paper has been peer-reviewed and accepted for publication, but has yet to undergo copyediting and proof correction. The final published version may differ from this proof.

However, at later stages (2-3 dpf), *glis3* morphants show a reduced or absent expression of *tg* and *slc5a5*, two of the key genes involved in thyroid hormone synthesis. As a consequence of these developmental defects, the *glis3* morphant larvae present thyroid hypoplasia, a reduced number of T4-producing follicles, and high levels of *thsba* at 5 dpf, thus recapitulating the primary hypothyroidism observed in NDH patients.

Importantly, because no variations in proliferation or apoptosis were detected under *glis3* knockdown in the region including the thyroid bud, our findings support the concept that *glis3* action is fundamental for the quantitative regulation of the amount of endodermal precursors committed to a thyroid fate. Consistently, the recovery of the thyroid phenotype in the rescue experiment, as well as the opposite variation in the number of thyroid cells and T4-production obtained through overexpression of the *glis3* mRNA, confirms that the gene dosage of *glis3* is critical for correct development and size definition of the zebrafish thyroid. These effects appear independent of the tsh/tshr signal since these transcripts can be detected in zebrafish from 40-42 hpf (24, 26), and tshba was found to be high in *glis3* morphants. Previous work on zebrafish *shh* mutants reported an impaired pituitary gland and absence of *tshba* positive cells (47-49). This discrepant effect on pituitary markers may perhaps be explained by the involvement of different downstream effectors of the Shh pathway in pituitary and thyroid development: Glis3 may have a more relevant role in thyroid (and endocrine pancreas) development, whereas other Gli-like factors may exert a main developmental role in the pituitary.

Interestingly, the pharyngeal endoderm appeared unaffected in *glis3* morphants (see Fig 4), thus excluding that the observed thyroid defects are a consequence of aberrant endoderm formation. Accordingly, we investigated whether other organs that arise from the endoderm (e.g. liver, exocrine and endocrine pancreas) display some developmental defects. Only the endocrine pancreas development appears to be affected by *glis3* knockdown, as *glis3* morphants display a reduced differentiation of the *ins2*-positive pancreatic β-cells that frequently fail to migrate and localize in a disorganized shape. This phenotype displays similarities with the previously reported alterations of endocrine pancreas differentiation in Glis3-deficient conditions (10, 18, 21, 50).

Thyroid
Glis3 as a critical regulator of thyroid primordium specification (DOI: 10.1089/thy.2019.0196)
This paper has been peer-reviewed and accepted for publication, but has yet to undergo copyediting and proof correction. The final published version may differ from this proof.

The decrease of the functional thyroid markers during *glis3* knockdown at 2-3 dpf could be the consequence of direct or indirect effects. Indeed, PAX8 and NKX2.1 were shown to regulate the transcription of thyroidal genes involved in thyroid hormone synthesis through the direct binding of their promoter regions (1, 2, 21), however CHIP-sequencing of mice thyroid tissues identified *Pax8*, *Pds*, and *Slc5a5* as direct transcriptional targets of Glis3, thus pointing to a direct regulatory role of Glis3 on thyroid function. In apparent contrast with our findings, transcriptome analysis showed that expression of *Pax8* and *Nkx2.1* was unchanged in Glis3KO mice one month after birth (21). This discrepancy might be explained by the existence of compensatory mechanisms (e.g. other Gli-like activities) that are able to rescue, at least partially, Glis3 deficiency in the murine thyroid. In partial agreement with our findings, Glis3KO pups tend to have smaller thyroid glands than wild-type littermates (21). In aggregate, these findings support the concept of a dual role for glis3 on thyroid gland activity by promoting its commitment from the pharyngeal endoderm and, later on, the function/proliferation of thyroid cells. Indeed, Glis3 was previously reported to have a dual role also in pancreatic function: a) by regulating the number of endocrine progenitors that will differentiate into β-cells during embryonic growth, and b) by postnatally mediating insulin secretion and β-cell proliferation (13-19, 51).

The post-translational stability and transcriptional activity of GLIS3 were reported to be regulated by the binding with the Suppressor of Fused (SUFU), a negative regulator of the Sonic-hedgehog (SHH) signaling (20, 52, 53). In absence of SHH, SUFU would anchor GLIS3 in the cytoplasm preventing its interaction with the ubiquitin ligase CUL3 and ITCH, thus protecting GLIS3 from proteasome degradation (20, 54). On the other hand, the GLIS3-SUFU complex was also reported to translocate into the nucleus, where it recruits and interacts with co-repressors, suppressing the transcription of some target genes (e.g. *Ins2*) (13, 17, 20, 55). Through *in vitro* experiments, we then found that the zebrafish proteins glis3 and sufu co-localized in the nuclei of transfected cells and precipitate together in a co-IP assay, thus confirming that the interplay between glis3 and shh signaling occurs also in zebrafish. Subsequently, we observed that the *shha* signal is significantly reduced in the pharyngeal endoderm of *glis3* morphants, and coherently, the expression of *glis3* is

Thyroid
Glis3 as a critical regulator of thyroid primordium specification (DOI: 10.1089/thy.2019.0196)
This paper has been peer-reviewed and accepted for publication, but has yet to undergo copyediting and proof correction. The final published version may differ from this proof.

abolished in shh-deficient embryos (*shha* morphants and cyclopamine-treated embryos). Altogether these data point to a relevant developmental role of the shha-glis3 pathway in the pharyngeal endoderm and suggest that shh activity would induce expression of glis3 in the zebrafish endoderm.

Moreover, embryos treated with the shha antagonist developed a thyroid phenotype characterized by reduced/absent expression of early and late markers, a phenotype similar to that described in *glis3* morphants. Interestingly, cyclopamine treatment also prevents the *tg* up-regulation induced by *glis3*-overexpression. Therefore, *glis3* appears to require an active Shh-signal for its function, likely acting as a downstream effector of the Shh-pathway during zebrafish thyroid development.

In conclusion, we propose that glis3 acts as an effector of the Shh-pathway with a critical role during embryonic thyroid development. In particular, our data provide significant insights into the signaling pathways involved in the induction of thyroid precursors from the undifferentiated endoderm. However, additional experiments are needed to characterize the molecular events linking the shh-glis3 pathway and the expression and action of early thyroid transcription factors. Our findings may provide an explanation for the frequent developmental thyroid defects in patients with *GLIS3* mutations. Finally, zebrafish may represent an alternative *in vivo* model suitable for high-throughput screening of drugs able to counteract GLIS3 deficiency (50).

Acknowledgments

The Authors wish to thank Dr Annamaria Maraschi (Milan) for the supply of pEGFP-C3 and pcDNA4-Myc/His constructs and for help with the setting of the experimental protocols for *in vitro* studies.

Correspondence: Prof Luca Persani, MD PhD; email: luca.persani@unimi.it

Author's Contributions and Disclosure Statement

GR designed and performed the *in vivo* experiments, and wrote the draft of the manuscript, and. FM supervised and contributed the zebrafish studies and the manuscript preparation. PD performed the *in vitro* experiments. LP conceived the study, obtained

research funds, revised and finalized the manuscript. All authors approved the final version of the manuscript.

The authors have declared that no conflict of interest exists

Funding: This work has been partially supported by the Ricerca Corrente funds of Istituto Auxologico Italiano, Milan, Italy (code: 05C102_2011) and by the PhD and Post-Doc programs of the University of Milan, Italy.

References

1. De Felice M, Di Lauro R 2004 Thyroid development and its disorders: genetics and molecular mechanisms. Endocr Rev **25**:722-746.

2. De Felice M, Di Lauro R 2007 Murine models for the study of thyroid gland development. Endocr Dev **10**:1-14.

3. Fagman H, Amendola E, Parrillo L, Zoppoli P, Marotta P, Scarfo M, De Luca P, de Carvalho DP, Ceccarelli M, De Felice M, Di Lauro R 2011 Gene expression profiling at early organogenesis reveals both common and diverse mechanisms in foregut patterning. Dev Biol **359**:163-175.

4. Szinnai G, Lacroix L, Carre A, Guimiot F, Talbot M, Martinovic J, Delezoide AL, Vekemans M, Michiels S, Caillou B, Schlumberger M, Bidart JM, Polak M 2007 Sodium/iodide symporter (NIS) gene expression is the limiting step for the onset of thyroid function in the human fetus. J Clin Endocrinol Metab **92**:70-76.

5. Persani L, Rurale G, de Filippis T, Galazzi E, Muzza M, Fugazzola L 2018 Genetics and management of congenital hypothyroidism. Best practice & research Clin Endocrinol Metab **32**:387-396.

6. Peters C, van Trotsenburg ASP, Schoenmakers N 2018 Diagnosis of endocrine disease: Congenital hypothyroidism: update and perspectives. Eur J Endocrinol **179**:R297-R317.

7. Dimitri P 2017 The role of GLIS3 in thyroid disease as part of a multisystem disorder. Best Pract Res Clin Endocrinol Metab **31**:175-182.

8. Senee V, Chelala C, Duchatelet S, Feng D, Blanc H, Cossec JC, Charon C, Nicolino M, Boileau P, Cavener DR, Bougneres P, Taha D, Julier C 2006 Mutations in GLIS3 are responsible for a rare syndrome with neonatal diabetes mellitus and congenital hypothyroidism. Nat Genet **38**:682-687.

9. de Filippis T, Gelmini G, Paraboschi E, Vigone MC, Di Frenna M, Marelli F, Bonomi M, Cassio A, Larizza D, Moro M, Radetti G, Salerno M, Ardissino D, Weber G, Gentilini D, Guizzardi F, Duga S, Persani L 2017 A frequent oligogenic involvement in congenital hypothyroidism. Hum Mol Genet **26**:2507-2514.

Thyroid
Glis3 as a critical regulator of thyroid primordium specification (DOI: 10.1089/thy.2019.0196)
This paper has been peer-reviewed and accepted for publication, but has yet to undergo copyediting and proof correction. The final published version may differ from this proof.

10. Jetten AM 2018 GLIS1-3 transcription factors: critical roles in the regulation of multiple physiological processes and diseases. Cell Mol Life Sci **75**:3473-3494.

11. Kim YS, Nakanishi G, Lewandoski M, Jetten AM 2003 GLIS3, a novel member of the GLIS subfamily of Kruppel-like zinc finger proteins with repressor and activation functions. Nucleic Acids Res **31**:5513-5525.

12. Lichti-Kaiser K, ZeRuth G, Jetten AM 2014 Transcription Factor Gli-Similar 3 (Glis3): Implications for the Development of Congenital Hypothyroidism. J Endocrinol Diabetes Obes **2**:1024.

13. Kang HS, Kim YS, ZeRuth G, Beak JY, Gerrish K, Kilic G, Sosa-Pineda B, Jensen J, Pierreux CE, Lemaigre FP, Foley J, Jetten AM 2009 Transcription factor Glis3, a novel critical player in the regulation of pancreatic beta-cell development and insulin gene expression. Mol Cell Biol **29**:6366-6379.

14. Watanabe N, Hiramatsu K, Miyamoto R, Yasuda K, Suzuki N, Oshima N, Kiyonari H, Shiba D, Nishio S, Mochizuki T, Yokoyama T, Maruyama S, Matsuo S, Wakamatsu Y, Hashimoto H 2009 A murine model of neonatal diabetes mellitus in Glis3-deficient mice. FEBS Lett **583**:2108-2113.

15. Yang Y, Chang BH, Chan L 2013 Sustained expression of the transcription factor GLIS3 is required for normal beta cell function in adults. EMBO Mol Med **5**:92-104.

16. Kang HS, Takeda Y, Jeon K, Jetten AM 2016 The Spatiotemporal Pattern of Glis3 Expression Indicates a Regulatory Function in Bipotent and Endocrine Progenitors during Early Pancreatic Development and in Beta, PP and Ductal Cells. PloS One **11**:e0157138.

17. Hang Y, Stein R 2011 MafA and MafB activity in pancreatic beta cells. Trends Endocrinol Metab **22**:364-373.

18. Yang Y, Chang BH, Samson SL, Li MV, Chan L 2009 The Kruppel-like zinc finger protein Glis3 directly and indirectly activates insulin gene transcription. Nucleic Acids Res **37**:2529-2538.

19. ZeRuth GT, Takeda Y, Jetten AM 2013 The Kruppel-like protein Gli-similar 3 (Glis3) functions as a key regulator of insulin transcription. Mol Endocrinol **27**:1692-1705.

20. ZeRuth GT, Yang XP, Jetten AM 2011 Modulation of the transactivation function and stability of Kruppel-like zinc finger protein Gli-similar 3 (Glis3) by Suppressor of Fused. J Biol Chem **286**:22077-22089.

Thyroid

Glis3 as a critical regulator of thyroid primordium specification (DOI: 10.1089/thy.2019.0196)

21. Kang HS, Kumar D, Liao G, Lichti-Kaiser K, Gerrish K, Liao XH, Refetoff S, Jothi R, Jetten AM 2017 GLIS3 is indispensable for TSH/TSHR-dependent thyroid hormone biosynthesis and follicular cell proliferation. J Clin Invest **127**:4326-4337.

22. Dimitri P, Habeb AM, Gurbuz F, Millward A, Wallis S, Moussa K, Akcay T, Taha D, Hogue J, Slavotinek A, Wales JK, Shetty A, Hawkes D, Hattersley AT, Ellard S, De Franco E 2015 Expanding the Clinical Spectrum Associated With GLIS3 Mutations. J Clin Endocrinol Metab **100**:E1362-1369.

23. Wendl T, Lun K, Mione M, Favor J, Brand M, Wilson SW, Rohr KB 2002 Pax2.1 is required for the development of thyroid follicles in zebrafish. Development **129**:3751-3760.

24. Porazzi P, Calebiro D, Benato F, Tiso N, Persani L 2009 Thyroid gland development and function in the zebrafish model. Mol Cell Endocrinol **312**:14-23.

25. Opitz R, Maquet E, Huisken J, Antonica F, Trubiroha A, Pottier G, Janssens V, Costagliola S 2012 Transgenic zebrafish illuminate the dynamics of thyroid morphogenesis and its relationship to cardiovascular development. Dev Biol **372**:203-216.

26. Opitz R, Antonica F, Costagliola S 2013 New model systems to illuminate thyroid organogenesis. Part I: an update on the zebrafish toolbox. Eur Thyroid J **2**:229-242.

27. Marelli F, Persani L 2017 How zebrafish research has helped in understanding thyroid diseases. F1000Res **6**:2137-2146.

28. Rurale G, Persani L, Marelli F 2018 GLIS3 and Thyroid: A Pleiotropic Candidate Gene for Congenital Hypothyroidism. Front Endocrinol (Lausanne) **9**:730-737.

29. Fishman MC, Stainier DY, Breitbart RE, Westerfield M 1997 Zebrafish: genetic and embryological methods in a transparent vertebrate embryo. Methods Cell Biol **52**:67-82.

30. Tsang B, Zahid H, Ansari R, Lee RC, Partap A, Gerlai R 2017 Breeding Zebrafish: A Review of Different Methods and a Discussion on Standardization. Zebrafish **14**:561-573.

31. Kimmel CB, Ballard WW, Kimmel SR, Ullmann B, Schilling TF 1995 Stages of embryonic development of the zebrafish. Dev Dyn **203**:253-310.

32. Marelli F, Carra S, Agostini M, Cotelli F, Peeters R, Chatterjee K, Persani L 2016 Patterns of thyroid hormone receptor expression in zebrafish and generation of a novel model of resistance to thyroid hormone action. Mol Cell Endocrinol **424**:102-117.

33. Alt B, Reibe S, Feitosa NM, Elsalini OA, Wendl T, Rohr KB 2006 Analysis of origin and growth of the thyroid gland in zebrafish. Dev Dyn **235**:1872-1883.

34. Opitz R, Maquet E, Zoenen M, Dadhich R, Costagliola S 2011 TSH receptor function is required for normal thyroid differentiation in zebrafish. Mol Endocrinol **25**:1579-1599.

35. diIorio P, Alexa K, Choe SK, Etheridge L, Sagerstrom CG 2007 TALE-family homeodomain proteins regulate endodermal sonic hedgehog expression and pattern the anterior endoderm. Dev Biol **304**:221-231.

36. Porazzi P, Marelli F, Benato F, de Filippis T, Calebiro D, Argenton F, Tiso N, Persani L 2012 Disruptions of global and JAGGED1-mediated notch signaling affect thyroid morphogenesis in the zebrafish. Endocrinology **153**:5645-5658.

37. Korzh V, Edlund T, Thor S 1993 Zebrafish primary neurons initiate expression of the LIM homeodomain protein Isl-1 at the end of gastrulation. Development **118**:417-425.

38. Odenthal J, Nusslein-Volhard C 1998 fork head domain genes in zebrafish. Dev Genes Evol **208**:245-258.

39. Zecchin E, Mavropoulos A, Devos N, Filippi A, Tiso N, Meyer D, Peers B, Bortolussi M, Argenton F 2004 Evolutionary conserved role of ptf1a in the specification of exocrine pancreatic fates. Dev Biol **268**:174-184.

40. Biemar F, Argenton F, Schmidtke R, Epperlein S, Peers B, Driever W 2001 Pancreas development in zebrafish: early dispersed appearance of endocrine hormone expressing cells and their convergence to form the definitive islet. Dev Biol **230**:189-203.

41. Thisse C, Thisse B 2008 High-resolution in situ hybridization to whole-mount zebrafish embryos. Nat Protocols **3**:59-69.

42. Lauter G, Soll I, Hauptmann G 2011 Two-color fluorescent in situ hybridization in the embryonic zebrafish brain using differential detection systems. BMC Dev Biol **11**:43-54.

43. O'Hare EA, Yerges-Armstrong LM, Perry JA, Shuldiner AR, Zaghloul NA 2016 Assignment of Functional Relevance to Genes at Type 2 Diabetes-Associated Loci Through Investigation of beta-Cell Mass Deficits. Mol Endocrinol **30**:429-445.

44. Zhang C, Ojiaku P, Cole GJ 2013 Forebrain and hindbrain development in zebrafish is sensitive to ethanol exposure involving agrin, Fgf, and sonic hedgehog function. Birth defects research Part A, Clinical and molecular teratology **97**:8-27.

Thyroid

Glis3 as a critical regulator of thyroid primordium specification (DOI: 10.1089/thy.2019.0196)

45. Chen JK, Taipale J, Cooper MK, Beachy PA 2002 Inhibition of Hedgehog signaling by direct binding of cyclopamine to Smoothened. Genes Dev **16**:2743-2748.

46. Incardona JP, Gaffield W, Kapur RP, Roelink H 1998 The teratogenic Veratrum alkaloid cyclopamine inhibits sonic hedgehog signal transduction. Development **125**:3553-3562.

47. Devine CA, Sbrogna JL, Guner B, Osgood M, Shen MC, Karlstrom RO 2009 A dynamic Gli code interprets Hh signals to regulate induction, patterning, and endocrine cell specification in the zebrafish pituitary. Dev Biol **326**:143-154.

48. Herzog W, Zeng X, Lele Z, Sonntag C, Ting JW, Chang CY, Hammerschmidt M 2003 Adenohypophysis formation in the zebrafish and its dependence on sonic hedgehog. Dev Biol **254**:36-49.

49. Sbrogna JL, Barresi MJ, Karlstrom RO 2003 Multiple roles for Hedgehog signaling in zebrafish pituitary development. Dev Biol **254**:19-35.

50. Amin S, Cook B, Zhou T, Ghazizadeh Z, Lis R, Zhang T, Khalaj M, Crespo M, Perera M, Xiang JZ, Zhu Z, Tomishima M, Liu C, Naji A, Evans T, Huangfu D, Chen S 2018 Discovery of a drug candidate for GLIS3-associated diabetes. Nat Commun **9**:2681-2693.

51. Yang Y, Bush SP, Wen X, Cao W, Chan L 2017 Differential Gene Dosage Effects of Diabetes-Associated Gene GLIS3 in Pancreatic beta Cell Differentiation and Function. Endocrinology **158**:9-20.

52. Li B, Rauhauser AA, Dai J, Sakthivel R, Igarashi P, Jetten AM, Attanasio M 2011 Increased hedgehog signaling in postnatal kidney results in aberrant activation of nephron developmental programs. Hum Mol Genet **20**:4155-4166.

53. Rual JF, Venkatesan K, Hao T, Hirozane-Kishikawa T, Dricot A, Li N, Berriz GF, Gibbons FD, Dreze M, Ayivi-Guedehoussou N, Klitgord N, Simon C, Boxem M, Milstein S, Rosenberg J, Goldberg DS, Zhang LV, Wong SL, Franklin G, Li S, Albala JS, Lim J, Fraughton C, Llamosas E, Cevik S, Bex C, Lamesch P, Sikorski RS, Vandenhaute J, Zoghbi HY, Smolyar A, Bosak S, Sequerra R, Doucette-Stamm L, Cusick ME, Hill DE, Roth FP, Vidal M 2005 Towards a proteome-scale map of the human protein-protein interaction network. Nature **437**:1173-1178.

Thyroid
Glis3 as a critical regulator of thyroid primordium specification (DOI: 10.1089/thy.2019.0196)
This paper has been peer-reviewed and accepted for publication, but has yet to undergo copyediting and proof correction. The final published version may differ from this proof.

54. ZeRuth GT, Williams JG, Cole YC, Jetten AM 2015 HECT E3 Ubiquitin Ligase Itch Functions as a Novel Negative Regulator of Gli-Similar 3 (Glis3) Transcriptional Activity. PloS One **10**:e0131303.

55. Chou CK, Tang CJ, Chou HL, Liu CY, Ng MC, Chang YT, Yuan SF, Tsai EM, Chiu CC 2017 The Potential Role of Kruppel-Like Zinc-Finger Protein Glis3 in Genetic Diseases and Cancers. Arch Immunol Ther Exp (Warsz) **65**:381-389.

Thyroid
Glis3 as a critical regulator of thyroid primordium specification (DOI: 10.1089/thy.2019.0196)
This paper has been peer-reviewed and accepted for publication, but has yet to undergo copyediting and proof correction. The final published version may differ from this proof.

Thyroid
Glis3 as a critical regulator of thyroid primordium specification (DOI: 10.1089/thy.2019.0196)

Figure Legends

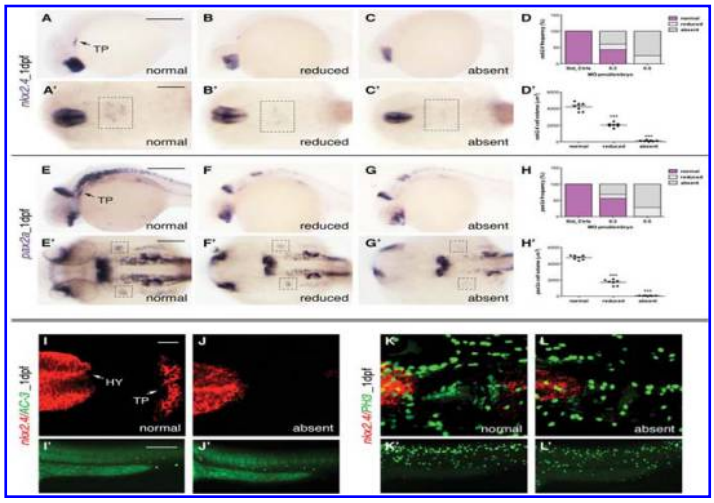

Figure 1. Analysis of the developing thyroid primordium (TP). (**A-C and A'-C'**) WISH of nkx2.4 expression in embryos injected with Std-CtrlMO and glis3MO_SPL at 0.3 and 0.5pmol/e. Images are representative of injected embryos that expressed normal, reduced or absent *nkx2.4* signal acquired in lateral and dorsal view. (**E-G and E'-G'**) *pax2a* expression in the injected embryos at 1dpf. The embryos were subdivided belonging the three phenotypic classes described above. Scale bar: 250µm. (**Graphs D, H**) Bars indicate the percentages of the injected embryos belonging the different phenotypic classes. (**Graphs D', H'**) Quantification of *nkx2.4* and *pax2a* at 1 dpf in the control and morphant embryos belonging the thyroid phenotypic classes. Data were obtained from 10 embryos for each class. Statistical significance was calculated using Student's t-test (***P<0.001). (**I-L**) WISH of nkx2.4, at 1dpf, using FastBlue staining for the acquisition of the fluorescence signal, followed by activated caspase-3 (AC-3) (**I-J**) and phospho-histone H3 (PH3) (**K-L**) immunostaining. Std-ctrl embryos reveal the correct development of the thyroid primordium. In glis3-morphants the thyroid primordium is absent. No differences in AC-3 or in PH3 immunostaining were observed in morphants, compared to controls. Embryos are all flat mounted, in ventral view, with the anterior to the left. Scale bar: 100 µm. (**I'-J'** and **K'-L'**) AC-3 and PH3 staining of the trunktail regions were used as control of experimental conditions. Each experiment was performed in triplicate, using 40 embryos per MO injected. HY: hypothalamus, TP:thyroid primordium.

Thyroid
Glis3 as a critical regulator of thyroid primordium specification (DOI: 10.1089/thy.2019.0196)
This paper has been peer-reviewed and accepted for publication, but has yet to undergo copyediting and proof correction. The final published version may differ from this proof.

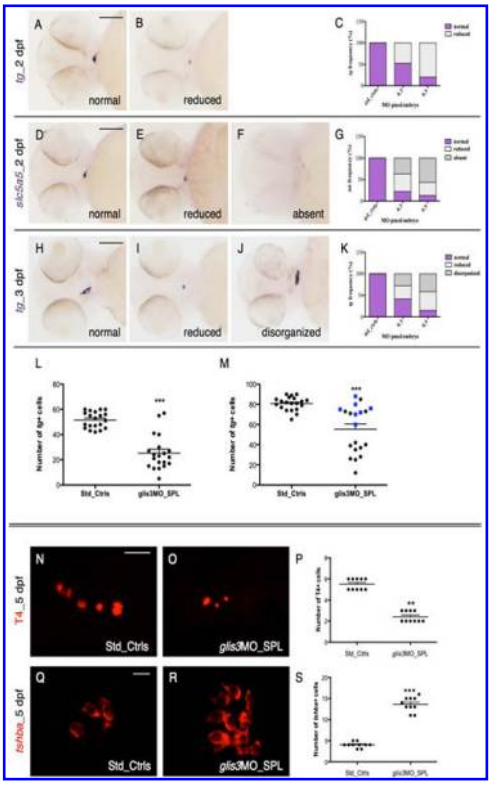

Fig 2. Analysis of development and function of thyroid gland. **A and B** WISH of *tg* expression in embryos injected with Std-ctrlMO and *glis3*MO_SPL at 0.3 and 0.5pmol/e, at 2dpf. **D-F** *slc5a5* expression in the injected embryos at 2 dpf. **H-J** analysis of thyroid elongation using WISH of *tg*, in the injected embryos at 3 dpf. **Graphs C, G and K** bars indicate the percentages of the injected embryos belonging the different phenotypic classes. **Graphs L and M** quantification of *tg* cell number in control and morphant embryos at 2 and 3 dpf. Blue squares indicate morphants with a disorganized thyroid. **N-O** anti-T4 IHC in control and in *glis3*MO_SPL larvae at 0.5 pmol/e, at 5 dpf. **P** count of the number of T4-producing follicles in Std_CtrlMO and in *glis3*MO_SPL injected larvae. **Q-R** WISH of *tshba* using FastBlue staining for the acquisition of the fluorescence signal in control and in *glis3*MO_SPL larvae at 0.5 pmol/e, at 5 dpf. **S** count of the number of *tshba*-producing follicles in Std_CtrlMO and in *glis3*MO_SPL injected larvae. Each experiment was performed in triplicate, using 40 embryos per MO injected. For quantification (P and S), 10 embryos were used for each injection. All views were acquired in ventral view, anterior to the left. Scale bars: 250 µm and100 µm. Statistical significance is calculated using Student's t-test (**p<0.01; *** p<0.001).

Thyroid
Glis3 as a critical regulator of thyroid primordium specification (DOI: 10.1089/thy.2019.0196)
This paper has been peer-reviewed and accepted for publication, but has yet to undergo copyediting and proof correction. The final published version may differ from this proof.

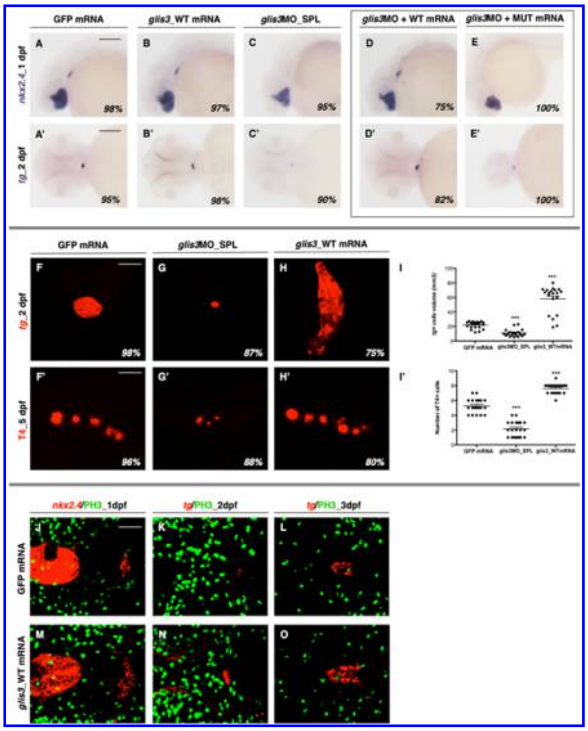

Fig 3. Rescue experiment. A-E' WISH of *nkx2.4* expression, at 1 dpf and *tg* at 2 dpf, in embryos injected with GFP mRNA (100 pg/e), *glis3*_WT mRNA (100 pg/e), *glis3*MO_SPL (0.5 pmol/e), *glis3*MO_SPL (0.5 pmol/e) + *glis3*_WT mRNA (100 pg/e), and *glis3*MO_SPL (0.5 pmol/e) + *glis3*_MUT mRNA (100 pg/e). Views of embryos were acquired in lateral (A-E) and ventral (A'-E') views, anterior to the left. Scale bar: 250 µm. **Analysis of *glis3* overexpression. F-H** WISH of *tg* using FastBlue staining for the acquisition of the fluorescence signal. **I** Quantification of the thyroid volume (mm^3) in 20 embryos injected with GFP mRNA (250 pg/e), *glis3*MO_SPL (0.5 pmol/e), and *glis3*_WT mRNA (250 pg/e). **F'-H'** Anti-T4 IHC in the injected larvae at 5dpf. **I'** count of the number of T4-producing follicles in 20 embryos injected for each condition. **J-L and M-O** WISH of *nkx2.4* and *tg*, using FastBlue staining for the acquisition of the fluorescence signal, followed by phospho-histone H3 (PH3) IHC.

Embryos were all flat mounted and acquired in ventral view, with the anterior to the left. Scale bar: 100 µm. *Asterisks* indicate statistically significant differences (Mann-Whitney test; ***, p<001).

Thyroid
Glis3 as a critical regulator of thyroid primordium specification (DOI: 10.1089/thy.2019.0196)

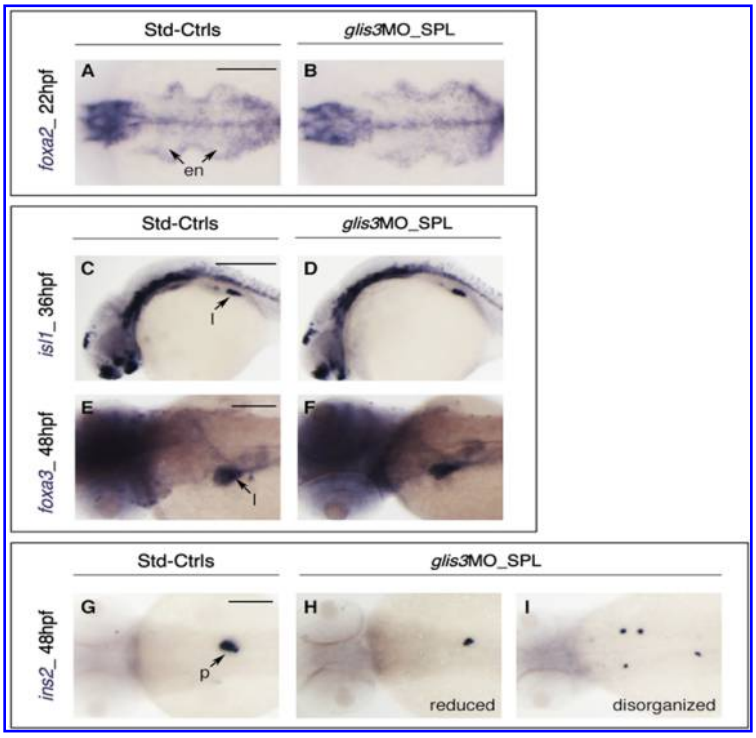

Fig 4. Analysis of pharyngeal endoderm and endoderm-derived organs in *glis3* morphants. A-B WISH showing *foxa2* expression in the endoderm (en) at 22 hpf. **C-F** analysis of liver (l) formation by WISH of (C-D) *isl1* at 36 hpf and (E-F) *foxa3* at 48hpf. **G-I** analysis of pancreas (p) development by WISH of *ins2* at 48hpf. Each experiment was performed in triplicate, using 35 embryos per MO injected. Views of embryos were acquired in dorsal (A-B, E-F and G-I) and lateral (C-D) view, anterior to the left. Scale bars: 250 µm and 100 µm.

Thyroid
Glis3 as a critical regulator of thyroid primordium specification (DOI: 10.1089/thy.2019.0196)

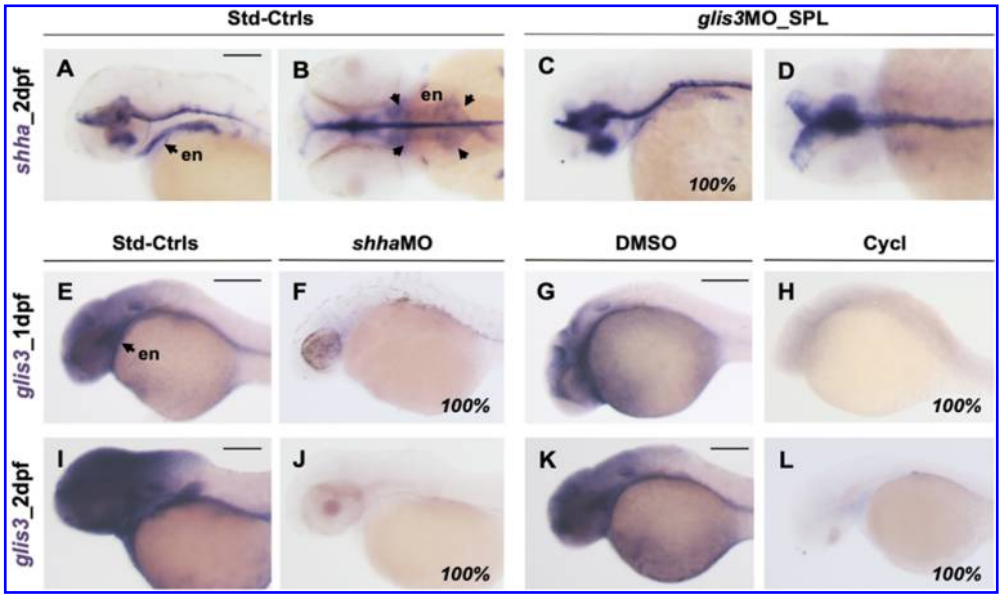

Fig 5. Analysis *shha* expression in *glis3* morphants. **A-D** WISH of *shha* expression in embryos injected with Std-ctrl and *glis3*MO_SPL at 0.5 pmol/e. **E-J** analysis *glis3* expression in *shh* deficient embryos. To blocking the activity of the Shh pathway, the *shha*_MO (1.25 pmol/e) and the pharmacological inhibitor cyclopamine (10µM) are used. As controls, embryos injected with Std_CtrlMO or treated with DMSO (vehicle) were used. Each experiment was performed in triplicate, using 50 embryos per each experiment. Embryos were acquired in lateral (A, C, E-L) and dorsal (B, D) views, anterior to the left. Scale bar: 250 µm. en: endoderm.

Thyroid
Glis3 as a critical regulator of thyroid primordium specification (DOI: 10.1089/thy.2019.0196)

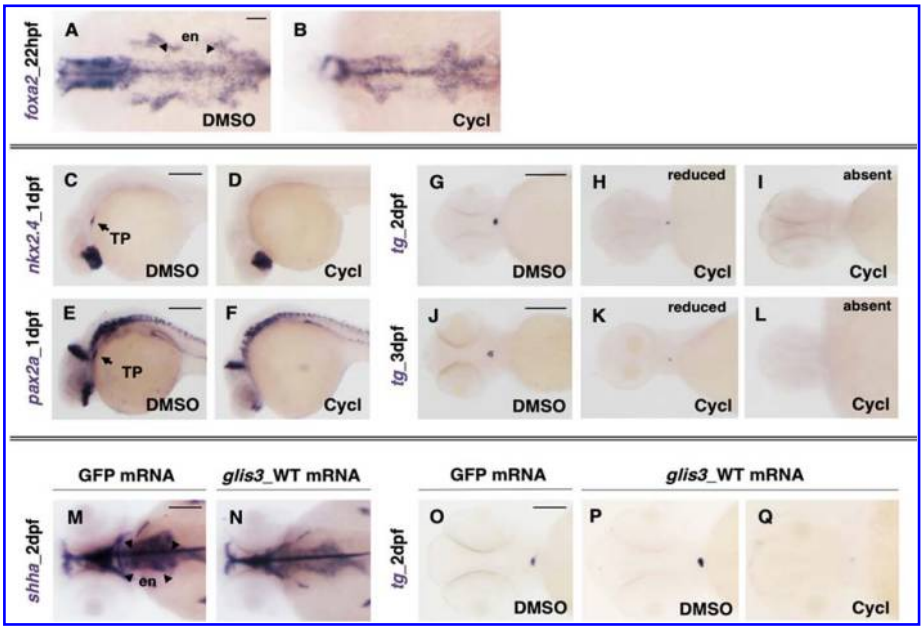

Fig 6. Analysis of thyroid gland development in cyclopamine-treated embryos. A and B WISH showing *foxa2* expression in the endoderm (en) at 22 hpf in control embryos (DMSO 1%) and embryos treated with cyclopamine (10µM)**. C-F** WISH of *nkx2.4* and *pax2a* expression at 1dpf. **G-L** WISH of *tg* at 2 and 3dpf. The embryos are subdivided as normal, reduced or absent *tg* signal. Analysis of *shha* in *glis3* overexpressing embryos. **M and N** WISH of *shha* expression in embryos injected with GFP mRNA (250 pg) and *glis3*_WT mRNA (250 pg/e) at 2dpf. Cyclopamine treatment in *glis3*-overexpressing embryos. **O-Q** WISH of *tg* in embryos injected with the GFP mRNA (250 pg) and the *glis3*_WT mRNA (250 pg/e), followed with treatment with DMSO or Cyclopamine (10 µM). Each experiment was performed in triplicate, using 50 embryos. Views of embryos were acquired in lateral (C-F), dorsal (A, B, M and N) and ventral (G-L and O-Q) views, anterior to the left. Scale bar: 250 µm.TP: thyroid primordium, en: endoderm.

1. Molecular and morphological validation of *glis3*MO_SPL

The *glis3*MO_SPL was designed to overlap with the exon2-intron2/3 boundary of the glis3 pre-mRNA, which resulted in the retention of a portion of the intron2/3. Different sets of primers were used to discriminate between the wild-type (mRNA-WT) and morphant (mRNA-MO) trancripts (Supplementary Fig 1A). The validation of morpholino performed by semiquantitave and qRT-PCR revealed that the amount of aberrant transcript (mRNA-MO) was dependent by the dose of *glis3*MO_SPL (0.3-1pmol/embryo) injected (Supplementary Fig 1B and C).

Thyroid
Glis3 as a critical regulator of thyroid primordium specification (DOI: 10.1089/thy.2019.0196)

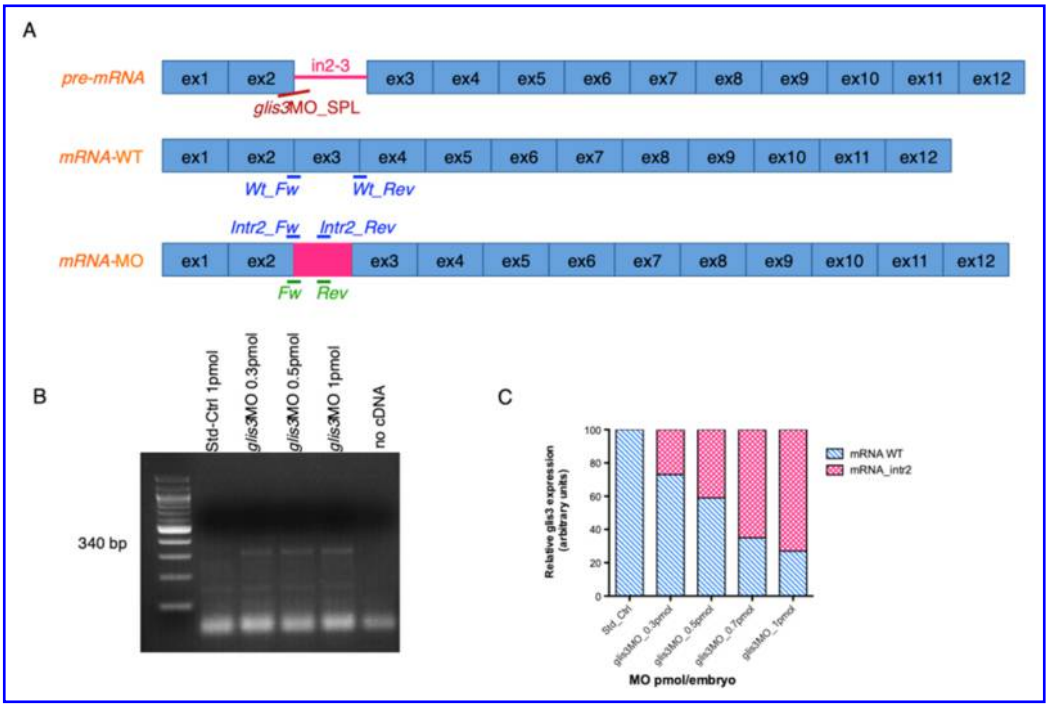

Supplementary Fig 1. Morpholino-mediated knockdown of the *glis3* genes in zebrafish. **A** *glis3* gene structure: the squared boxes correspond to the exons, the orange lines correspond to the introns. *glis3*SPL_MO is targeted to the splice donor site between exon 2 and intron 2-3 (E2i2-3). The position of primer sets used in RT-PCR and qRT-PCR to analyse the altered splicing are indicated in green and in blue, respectively. **B** The *glis3*MO_SPL was validated by RT-PCR injecting different doses (0.3, 0.5, 0.7 and 1pmol/ embryo) in the zebrafish embryos at 1-2 cells stage. The *glis3*SPL_MO causes the retention of a part of intron2-3 producing a PCR product of 340bp. **C** qRT-PCR of WT (mRNA WT) and aberrant (mRNA_intr2) glis3 transcripts expressed after injec- tion of growing doses of *glis3*MO_SPL.

Subsequently, to chose the working doses of MO, we analyzed different morphological parameters (embryonic length, tail curvature, cardiac edema, and head necrosis). At 1-3 dpf, the embryos were observed and classified into three different phenotypic classes (Supplementary Fig2): normal (Panels B, F, and L), similar to embryos injected with the Std-CtrlMO (Panels A, E, and I); moderate (Panels C, G, and M), presenting slight alterations in body-length and tail curvature, small head and cardiac edema; severe (Panels D, H, and N), with gross morphological alterations, and extensive necrosis.

The 0.3 and 0.5pmol/embryos were selected for the further experiments, because the severe class was less represented (Graph O).

Thyroid
Glis3 as a critical regulator of thyroid primordium specification (DOI: 10.1089/thy.2019.0196)
This paper has been peer-reviewed and accepted for publication, but has yet to undergo copyediting and proof correction. The final published version may differ from this proof.

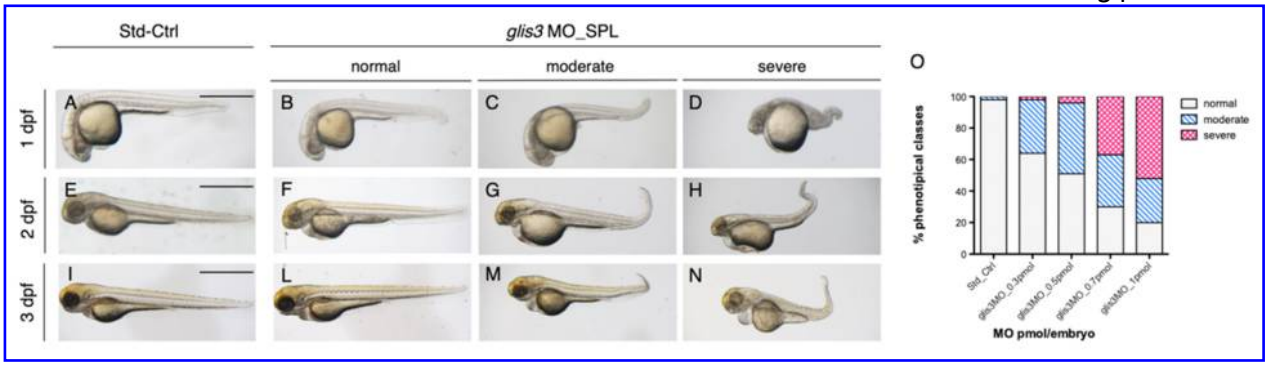

Supplementary Fig 2. Phenotypic classes of embryos injected with *glis3*MO_SPL. **A-N** Three phenotypic classes normal, moderate and severe analysed at three different developmen- tal stages (1, 2, and 3 dpf). The normal embryos (B, F and L) are indistinguishable form the controls (A, E and I). The moderate class (C, G and M) presents embryos with curved tail, cardiac edema and impaired circulation. The severe embryos (D, H and N) are strongly affected by necrosis, car- diac edema, reduced circulation and stasis. **Histogram O** Frequency of the morphants belonging these phenotypic classes according to the in- jected doses. Scale bar: 250µm.

2. Double fluorescent analysis of the early anche late thyroid markers

Taking into account that the possible embryonic delay of morphants can influence the analysis, we evaluated the frequency of thyroid phenotypes at different time points. The percentage of embryos reaching the 26hpf or 30hpf with undetectable expression of *nkx2.4* and *pax2a* passed from 75-85% to 33-10%. Consequently at 30hpf, the embryos with reduced but detectable expression of both markers represented the most frequent phenotypic class (Fig 3A and B), likely due to a selection bias among the morphants. However, a reduced *tg* signal was seen in almost 100% of morphants at later stages (Fig 2). In this class of morphants, when the double WISH was performed, *pax2a* signal was affected to a larger extent than *nkx2.4* (Fig 3D and D'), but 75% of morphants displayed a significant reduction of both transcripts (Fig 3E and E'). In contrast with the diffuse co-localization in Std-Ctrls (Fig 3A''), only few cells co-expressed *nkx2.4* and *pax2a* in morphants (Fig 3D'' and E'').

Thyroid
Glis3 as a critical regulator of thyroid primordium specification (DOI: 10.1089/thy.2019.0196)

Between 55 and 60hpf, we observed similar thyroid phenotypic frequencies in morphants, consistent with the recovery of the developmental embryonic delay (Fig 3 F, G, K and L). At 60hpf, *nkx2.4* and *tg* signals were reduced to variable extent in 45% of morphants, (Fig 3 I, I', H H'). However, a strong reduction of both signals was seen in the remaining 55% of morphants (Fig 3J and J'). The *pax2a* expression was always diminished in almost 100% of morphants (Fig 3N and O) associated with a variable decrease of *tg* (Fig 3N' and O'). In *glis3* morphants, the co-localization of *nkx2.4*/*tg* or *pax2a*/*tg* staining was almost undetectable (Fig 3H''-J'' and M''-O'').

Thyroid
Glis3 as a critical regulator of thyroid primordium specification (DOI: 10.1089/thy.2019.0196)
This paper has been peer-reviewed and accepted for publication, but has yet to undergo copyediting and proof correction. The final published version may differ from this proof.

Thyroid

Glis3 as a critical regulator of thyroid primordium specification (DOI: 10.1089/thy.2019.0196)

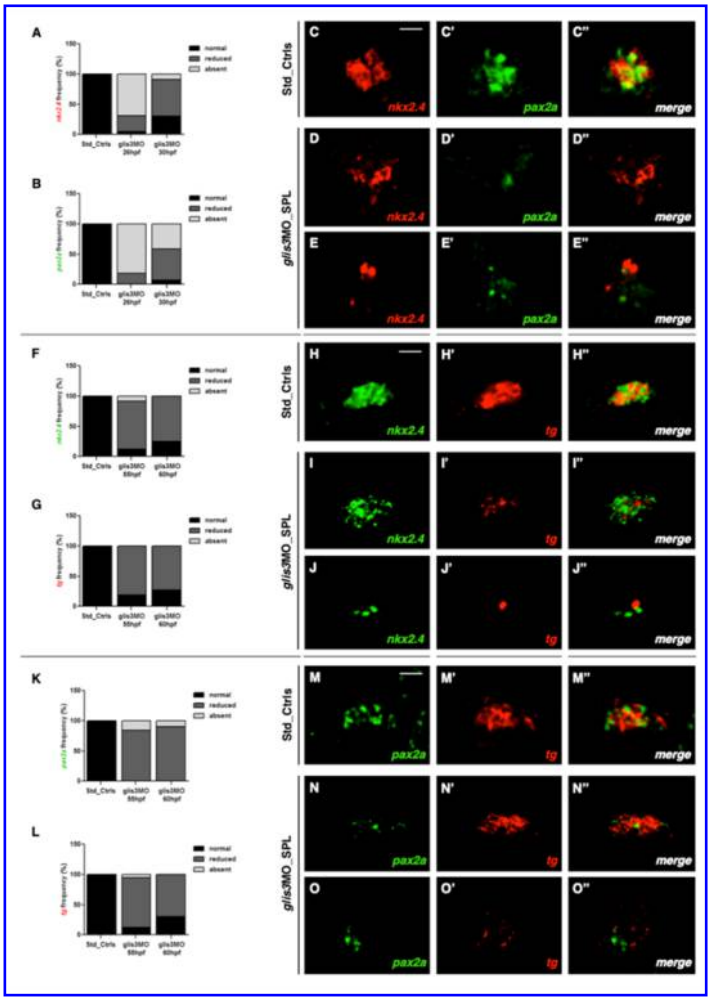

Supplementary Fig 3. **Double fluorescent WISH of thyroid markers. Graphs A-B, F-G, K-L** bars indicate the percentages of the injected embryos belonging the different phenotypic classes. **C-E''** nkx2.4/pax2a in Std_Ctrls at 26hpf and glis3 morphants at 30hpf. H-J'' nkx2.4/tg in Std_Ctrls at 55hpf and glis3 morphants at 60hpf. **M-O''** pax2a/tg in Std_Ctrls at 55hpf and glis3 morphants at 60hpf. All embryos are acquired in ventral view, anterior to the top. Scale bar: 100µm. The images are representative of 10 embryos per injection performed in triplicate.

3. Molecular and morphological analysis of the alternative *glis3*MO2

The second *glis3*MO_SPL (*glis3*_MO2) was designed to overlap with the intron3/exon4 boundary of the glis3 pre-mRNA, which resulted in the skipping of the exon 4. (Ref. 33, O'Hare *et al*., 2016).

The morphological evaluation of the embryos injected with *glis3*_MO2 was performed as described before. The 0.7 pmol/embryos was selected for the further experiments, because the moderate class was well represented compared to normal and severe ones (Graph 4A).

As for the first *glis3*MO_SPL, we analysed the thyroid primordium development and function injected with 0.7pmol/e of *glis3*_MO2 (Graph 4B-E). Notably all the obtained results well recapitulated what was obtained with the first MO. In fact, at 1dpf the *glis3*_MO2 morphants exhibited a deficient formation of thyroid primordium with a marked reduction/absent expression of both *nkx2.4* and *pax2a* in most of the analysed embryos (4B). At 2dpf also the *tg* and *slc5a5* expression was reduced or absent in the morphants (4C). Consistently, at 5 dpf, the number of T4-positive follicles was significantly reduced in morphants compared to controls (4D), associated with an increased number of the tshba-positive pituitary cells (4E).

Thyroid
Glis3 as a critical regulator of thyroid primordium specification (DOI: 10.1089/thy.2019.0196)

Thyroid

Glis3 as a critical regulator of thyroid primordium specification (DOI: 10.1089/thy.2019.0196)

This paper has been peer-reviewed and accepted for publication, but has yet to undergo copyediting and proof correction. The final published version may differ from this proof.

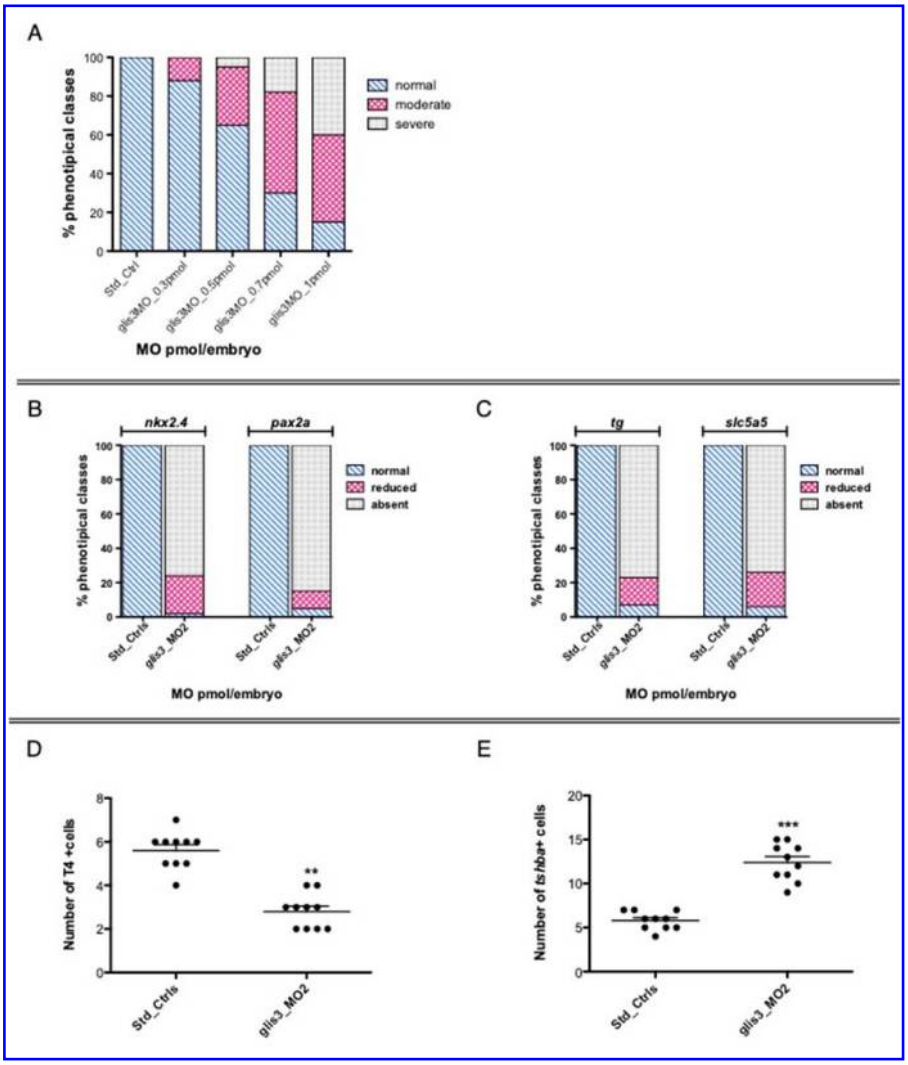

Supplementary Fig 4. Graph A Frequency of the phenotypic classes of embryos injected with *glis3*MO_2. **Graph B and C** Bars indicated the percentage of the *glis3*MO_2 injected embryos (0.7pmol/e) belonging the different phenotypic classes after WISH analysis of *nkx2.4*, *pax2a* at 1dpf (B) and *tg* and *slc5a5* at 2dpf (C). **Graph D and E** Count of the number of T4-positive cells (D) and tshba-producing follicles (E) in Std_Ctrls and *glis3*_MO2 injected larvae. Statistical significance is calculated using Student's t-test (**p <0.01; *** p<0.001).

4. Analysis of the pancreatic acini development in the glis3 knockdown embryos

In order to exclude a global impairment of the exocrine pancreas in the *glis3* morphants, we analysed the expression of *ptf1a*, a specific pancreatic acini transcription factor

(Supplementary Fig.5). The WISH analysis showed that the pancreatic acini were unaffected in the morphants (D) compared to controls (B), thus supporting the idea that *glis3* is specifically involved in the endocrine pancreas development.

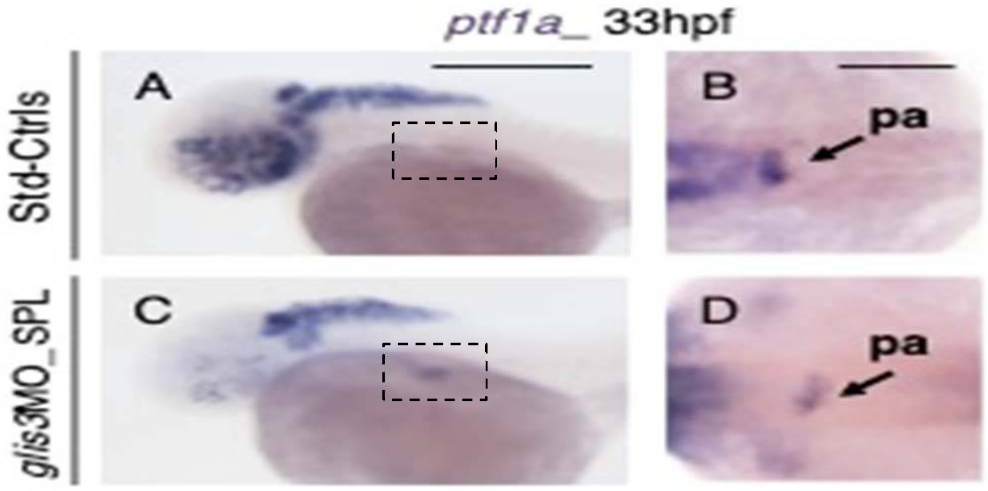

Supplementary Fig 5. Analysis of pancreatic acini development. (A-D) WISH of *ptf1a* expression in embryos injected with Std_CtrlMO and *glis3*MO_SPL at 0.5pmol/e at 33hpf. The signal was acquired in lateral (A and C) and dorsal (B and D, at higher magnification of the area of interest) view, anterior to the left. Scale bars: 250 and 100µm. pa: pancreatic acini.

5. glis3 and sufu zebrafish proteins interact *in vitro*

To test whether and how the glis3 and sufu zebrafish proteins interact, we performed an immune-localization and co-immuno-precipitation (Co-IP). In single transfection experiments, the pcDNA4-Myc/His-glis3 localized into the nucleus (Supplementary Fig 6A-C) whereas the pEGFP-sufu is visible in the cytosol (Fig 6D-F). Interestingly, both proteins co-localized into the nucleus of co-transfected HeLa cells (Fig 6G-I). The Co-IP assay confirmed that sufu and glis3 co-immunoprecipitate (Fig 6J) in a protein complex. Given the high conservation of the VYGHF motif at the N-terminus of zebrafish glis3, which is known to account for the sufu binding (44), the direct interaction of these two zebrafish proteins acquires likelihood.

Thyroid
Glis3 as a critical regulator of thyroid primordium specification (DOI: 10.1089/thy.2019.0196)
This paper has been peer-reviewed and accepted for publication, but has yet to undergo copyediting and proof correction. The final published version may differ from this proof.

Thyroid
Glis3 as a critical regulator of thyroid primordium specification (DOI: 10.1089/thy.2019.0196)

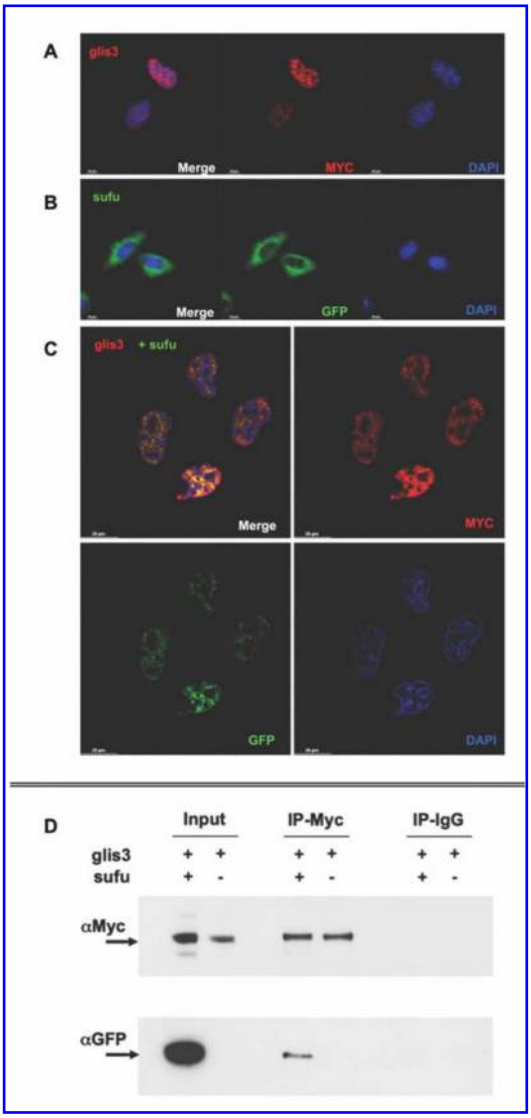

Supplementary Fig 6. **Immunolocalization of the zebrafish glis3 and sufu proteins. A-C and D-F** immunocytochemistry (ICC) of pcDNA4-Myc/His-glis3 and pEGFP-sufu individually transfected in HeLa cells. Glis3 colocalizes with dapi into the nucleus (C), whereas sufu presents a cytoplasmatic localization (F). **G-I** when cotransfected glis3 and sufu colocalize into the nucleus (I). **J** co-immunoprecipitation assay HeLa cells are transfected with pcDNA4-Myc/His-glis3 + pEGFP-sufu or with the glis3 plasmid alone. For each transfection the total protein content (input) and the immunoprecipitated for c-Myc or IgG (negative control) are subjected to WB analysis. The incubation with the anti-cMyc and anti-GFP antibodies is used to detect glis3 and sufu respectively.